Reaction of Acetaldehyde with Ni^+: An Extended Theoretical Study of the Decarbonylation Mechanism of Acetaldehyde by First-Row Transition Metal Ions

Xiangfeng Chen, Wenyue Guo,* Lianming Zhao, Qingtao Fu, and Yan Ma

College of Physics Science and Technology, China University of Petroleum, Dongying, Shandong 257061, People's Republic of China

Received: October 9, 2006; In Final Form: February 15, 2007

We report herein a theoretical study of the reaction of acetaldehyde with Ni^+ as an extension of our two recent papers on the decarbonylation of acetaldehyde by late first-row transition metal ions [Zhao, Zhang, Guo, Wu, Lu *Chem. Phys. Lett.* **2005**, *414*, 28; Zhao, Guo, Zhang, Wu, Lu *ChemPhysChem* **2006**, *7*, 1345]. Geometries of all the stationary points involved in the reaction have been fully optimized at the B3LYP/6-311+G(2df,2pd) level and the decarbonylation mechanism is analyzed in terms of the topology of potential energy surface. Combining with the previous studies, it is found that for the Cr^+, Co^+, and $^4Fe^+$ mediated systems decarbonylation of CH_3CHO only takes place via C−C activation, and aldehyde C−H activation is unlikely to be important, whereas both C−C and aldehyde C−H activations by Ni^+ and $^6Fe^+$ could result in the decarbonylation of CH_3CHO, where hydride-containing species $M^+(H)(CO)(CH_3)$ is found to be a common minimum along the reaction pathways.

1. Introduction

Recently, we[1,2] have theoretically investigated the gas-phase reaction of acetaldehyde with Co^+, Cr^+, and Fe^+ to unveil the first-row transition metal ions mediated decarbonylation mechanism that has been experimentally studied earlier.[3−7] Our results show that for Co^+, Cr^+, and $^4Fe^+$ the decarbonylation proceeds through C−C activation rather than aldehyde C−H activation and the reaction takes place through four elementary steps: encounter complexation, C−C activation, concerted aldehyde-H shift, and nonreactive dissociation, while the chemistry of $^6Fe^+$ with acetaldehyde involves a different, stepwise aldehyde-H-shift (two-step) mechanism, i.e., an aldehyde H-shift for the formation of hydride-containing species $(CH_3)M^+H(CO)$ and a subsequent hydride-H shift to form exit-channel species (CH_4)-$M^+(CO)$. It seems that the above-mentioned difference is dictated by the hydride-containing species. For instance, it is really a local minimum on the $^6Fe^+/CH_3CHO$ potential energy surface (PES), whereas for the Co^+, Cr^+, and $^4Fe^+/CH_3CHO$ systems no such a minimum could be found. In spite of the knowledge of the decarbonylation mechanism that has already been obtained, basic questions that still should be addressed are whether only C−C activation plays a role in the decarbonylation of acetaldehyde with first-row transition metal ions and in which situations C−H activation would result in decarbonylation products.

To answer these questions, in this paper, we extend our theoretical work to the chemistry of Ni^+ with acetaldehyde, which has been confirmed with an ion beam apparatus to give exclusively the decarbonylation products ($CH_4 + Ni^+(CO)$).[7] The structures of the involved species and the corresponding PES are studied in detail.

2. Computationa1 Details

The density functional method in its three-parameter hybrid B3LYP functional[8,9] was employed in conjunction with the 6-311+G(2df,2pd) basis set. This approach has been valuated to be of good validity for the Ni^+-containing system in previous papers.[10] The structures of all the reactants, products, intermediates, and transition states involved in the title reaction were fully optimized at the B3LYP/6-311+G(2df,2pd) level of theory. Frequency calculations were carried out at the same level to identify the stationary points optimized (minima or transition states) and to estimate zero-point energy (ZPE) corrections that are applied to all the reported energies. To confirm the transition states and their connected minima, intrinsic reaction coordinate (IRC) calculations were performed to follow the reaction pathways.[11] A full natural bond orbital (NBO) analysis was also carried out for some important stationary points to gain a further insight into the bonding properties.[12−14] We also detected the values of $\langle S^2 \rangle$ for all the calculated species to evaluate if spin contamination can influence the quality of the results and found it is less than 5% (see Table 1), suggesting spin contamination is small in all of the calculations. All the calculations were carried out with the Gaussian 03 package.[15]

3. Results and Discussion

Optimized geometries as well as structural parameters for the reactants, intermediates, and products involved in the title reaction at the B3LYP/6-311+G(2df,2pd) level are shown in Figure 1, tabulated in Table 1 are energies for these species, and Figure 2 gives the corresponding PES. It can be found that the reaction starts with formation of the encounter complexes of Ni^+ with acetaldehyde. Once the encounter complexes are formed, both C−C and aldehyde C−H insertions can convert the system into hydride-containing species **4**, which is followed by a H-shift and a subsequent nonreactive-dissociation giving rise to the decarbonylation products of $CH_4 + Ni^+(CO)$. In the following we will first present the theoretical results of the encounter complexes and then discuss the decarbonylation mechanism in detail.

As shown in Figure 1, interaction of Ni^+ (^2D) with acetaldehyde leads to two isomeric encounter complexes (*cis*- and *trans*-**1**), in accordance with the situation of acetaldehyde

10.1021/jp066616d CCC: $37.00
Published on Web 04/14/2007

TABLE 1: Calculated Energies, *E*, Zero-Point Energies, ZPEs (hartree), and $\langle S^2 \rangle$ for All the Species Involved in the Decarbonylation of Acetaldehyde by Ni^+ at the B3LYP/6-311+G(2df,2pd) Level of Theory

species	$\langle S^2 \rangle^{a,b}$	*E*	ZPE[c]
$Ni^+(^2D) + CH_3CHO$	0.75 + 0.0	−1661.85201	0.05312
trans-**1**	0.75	−1661.93847	0.05478
cis-**1**	0.75	−1661.93740	0.05499
2	0.78	−1661.87964	0.04963
3	0.78	−1661.86937	0.05061
4	0.79	−1661.84318	0.04588
5	0.75	−1661.95499	0.05136
$\mathbf{TS_1}-\mathbf{2}$	0.76	−1661.87856	0.04891
$\mathbf{TS_1}-\mathbf{3}$	0.76	−1661.86287	0.05111
$\mathbf{TS_2}-\mathbf{4}$	0.76	−1661.84080	0.0469
$\mathbf{TS_3}-\mathbf{4}$	0.77	−1661.84304	0.04525
$\mathbf{TS_4}-\mathbf{5}$	0.77	−1661.84169	0.04453
$Ni^+CH_4 + CO$	0.75 + 0.00	−1661.89061	0.04885
$Ni^+CO + CH_4$	0.75 + 0.00	−1661.91864	0.04938

[a] The expectation value of S^2 before annihilation. [b] The first number corresponds to the first species, and the second one to the second species. [c] ZPE corrections have not been taken into account.

complexes with Co^+ and Cr^+ but unlike that of Fe^+-acetaldehyde complexes, for which only the trans form was found on both the quartet and sextet PESs.[1,2] Both the Ni^+-acetaldehyde isomers ($^2A'$) are formed by the linkage of the metal ion to the O atom of acetaldehyde favored by an overall C_s symmetry with the symmetry plane defined by $O-C^1-Ni^+-C^2$. The absolute energies of the two isomers are nearly the same (the trans form is only 0.8 kcal/mol more stable than the cis conformer), indicating coexistence of them in the gas phase. For the isomers, the equilibrium Ni^+-O distances are almost identical (1.884−1.883 Å). Accordingly, nearly a same Ni^+-O binding energy is found (53.2 kcal/mol for *trans*-**1** and 52.4 kcal/mol for *cis*-**1**). Upon binding with Ni^+, the largest change in CH_3CHO is the increase in $O-C^1$ bond length (by 2.3−2.5%) as a result of oxygen polarizing charge toward Ni^+.

Similar to the situation of Co^+, Cr^+, and Fe^+,[1,2] C−C activation of *cis*-**1** can result in species **2** ($^2A'$), in which the nickel ion has been inserted into the C−C bond of acetaldehyde as reflected by the substantially stretched bond length (2.994 Å). The new intermediate is also featured by an overall C_s symmetry with $O-C^1-Ni^+-C^2$ as the symmetry plane as well as by nearly the same Ni^+-C distances (1.917−1.918 Å), suggesting the interaction of Ni^+ with the CH_3 and CHO groups is comparable. Energetically, this complex is calculated to be 12.5 kcal/mol more stable than the entrance channel or 39.9 kcal/mol less stable than *cis*-**1**.

$\mathbf{TS_{1-2}}$ connects *cis*-**1** and **2**, which has been confirmed by IRC calculations. The C^1-C^2 bond of $\mathbf{TS_{1-2}}$ is stretched to 2.143 Å, indicating the breaking of the bond. It can be found that $\mathbf{TS_{1-2}}$ takes a large structural similarity to **2**, thus it is indeed a late transition state on the PES. Accordingly, the transition state lies 44.3 and 4.4 kcal/mol respectively above the connected intermediates *cis*-**1** and **2**, or 8.1 kcal/mol lower in energy than the separated reactants.

Along the reaction coordinate, the C−C activation is followed by a stepwise (two-step) H-shift to form $Ni^+(CO)(CH_4)$ (**5**), the exit-channel complex. The first H-shift step involves an aldehyde H migration onto the metal center that destabilizes the system by 13.5 kcal/mol, leading to intermediate **4** (Ni^+-(H)(CO)(CH_3)). A striking feature of this new intermediate is the tricoordination of Ni^+ with CO, H, and CH_3, favored by an umbrella structure possessing no symmetry element other than C_1. Note that such a tricoordinated minimum was not found in the decarbonylation of acetaldehyde by Co^+, Cr^+, and $^4Fe^+$, where initial C−C activation is followed by a concerted H-shift process to form the decarbonylation precursor of $M^+(CO)(CH_4)$.[1,2] Earlier electronic structure studies also consistently failed to find potential minima corresponding to $M^+(H)(CH_3)(C_2H_4)$ and $M^+(H)_2(C_2H_4)$ (M = Fe, Co, and Ni).[16−18] Interestingly, we did identify such an analogous minimum as $Ni^+(CO)(CH_3)_2$ and $^6Fe^+(H)(CO)(CH_3)$, the later of which has a planar-skeleton structure rather than an umbrella structure as located for the analogous Ni^+-containing species.[2,10] As will be discussed below, this type of species is a common minimum on both C−C and aldehyde C−H activation pathways of acetaldehyde by metal ions.

One important question is why the tricoordinated minimum can only be located for some special metal ions, such as $^6Fe^+$ and Ni^+. It is expected that the existence of the minimum is determined by the stability of them, which depends on the bond strength of the three connected groups (H, CO, and CH_3) with metal center as well as the repulsion between the connected groups. For $^6Fe^+$, the $3d^64s^1$ electronic configuration would result in a $sd_{xz}d_{z^2-x^2}d_{y^2}$ (sd^3) hybridization of the metal β-orbitals to form the respective bonding orbital with H, CO, and CH_3 and a lone pair of the metal (where the C_s symmetry plane is defined by the *xz* coordinates with the *z*-axis polarized along CO), which then leads to the planar-skeleton structure as reported previously.[2] This structural feature not only strengthens the bonding interaction between the metal and the connected groups as discussed in ref 2 but also reduces the repulsion between the groups to the largest extent, leading to a quite stable tricoordinated minimum on the sextet $[Fe, C_2, H_4, O]^+$ PES.[2] For Ni^+, NBO calculations indicate that when binding with H, CO, and CH_3 the metal ($3d^9$) will experience a $4s3d^5$ hybridization to form the respective α-bonding orbitals with H and CO (leaving four metal orbitals as lone pairs) as well as the respective β-bonding orbitals with H, CO, and CH_3 (leaving three lone pairs on the metal). This type of hybridization could help the metal bond nicely with three radicals in a fully coordinated fashion, which stabilizes the system to some extent. However, the umbrella structure (see Figure 1) arising from the sd^5 hybridization of the metal destabilizes the species as indicated in Figure 2 that there is a very shallow region on the PES corresponding to $\mathbf{TS_{3-4}} \rightarrow \mathbf{4} \rightarrow \mathbf{TS_{4-5}}$. For the other metal ions, the inability to find the species may be due to the fact that the surface is very shallow and it is difficult to locate them or that it is indeed not a local minimum.

The conversion of **2** to **4** is through transition state $\mathbf{TS_{2-4}}$. The corresponding imaginary frequency of this transition state is 342*i* cm^{-1} and the normal mode of the vibration corresponds to the shift of the hydrogen atom onto the metal ion and the formation of the Ni^+-H bond. This transition state takes a large structural similarity to **4**, suggesting it is very "late" on the PES. Correspondingly, $\mathbf{TS_{2-4}}$ is located at 0.3 kcal/mol below **4** due to the ZPE effect, and 13.2 and 0.7 kcal/mol respectively above **2** and the separated reactants.

The metal-H migration that stabilizes the system by as much as 66.7 kcal/mol can convert complex **4** to **5**, the precursor species. This new species has an overall C_{2v} symmetry, and the methane moiety is found to be η^2 coordinated to the nickel ion, similar to the theoretical finding of $(CH_4)Co^+(CO)$.[1] NBO analysis shows that in the species the $4s_{Ni^+}$ orbital and the $2p_x$ orbital of C_1 form a σ_{Ni^+C} bonding orbital (where the *x*-axis polarizes along CO), while the linkage of methane with Ni^+ is strengthened by donations from both the coordinated bonds into the $\sigma^*_{Ni^+C}$ orbital. The structure of the $Ni^+(CO)$ group of **5** is almost identical with that of free $Ni^+(CO)$, and the respective

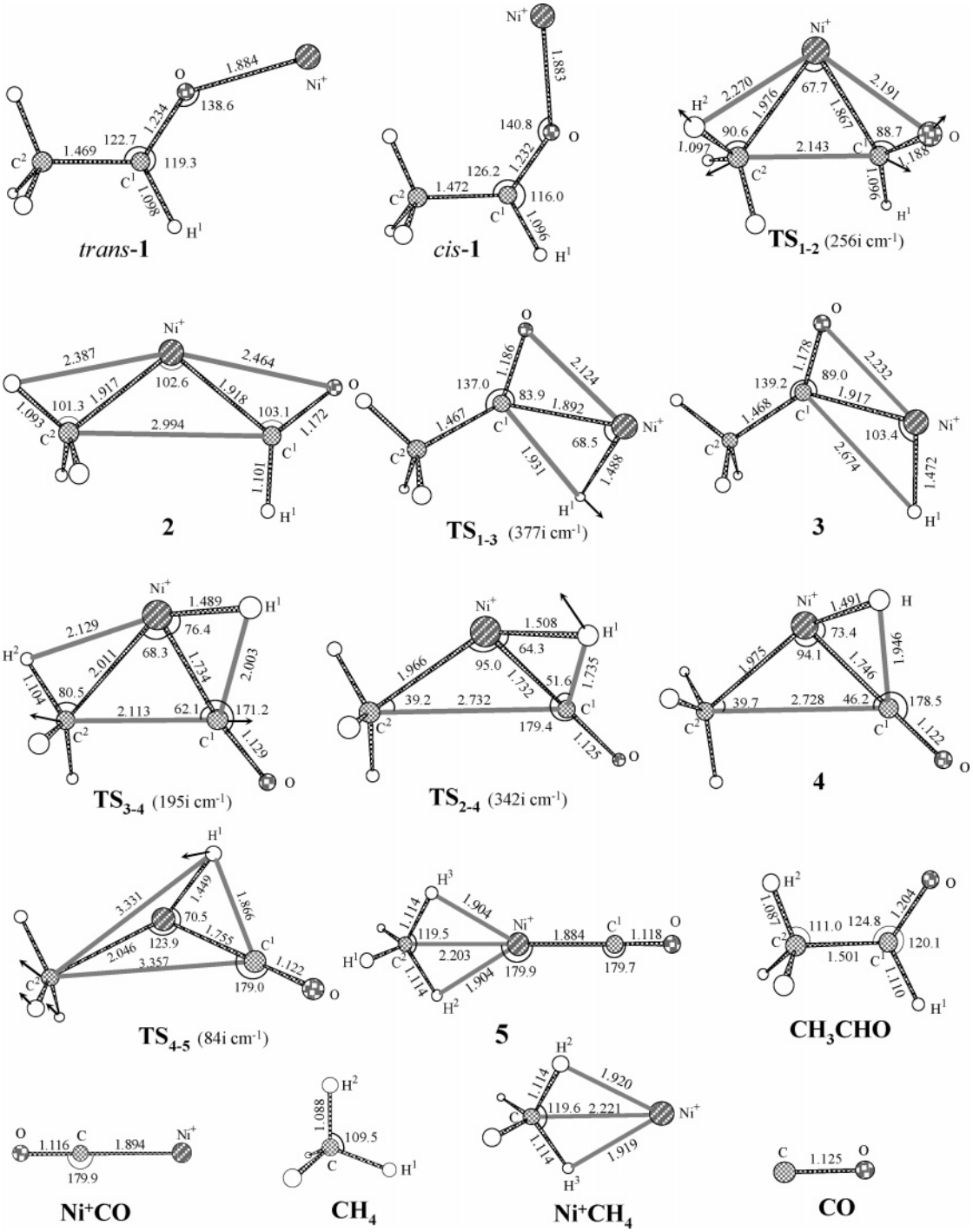

Figure 1. Optimized geometries and selected structural parameters at the B3LYP/6-311+G(2df,2pd) level of theory for the reactants, products, intermediates, and saddle points involved in the decarbonylation of acetaldehyde with Ni^+. Bond lengths are in angstroms and bond angles in degrees.

Ni^+-C^2, Ni^+-H^2, and Ni^+-H^3 distances are calculated to be 2.203, 1.904, and 1.905 Å. Accordingly, the $H_4C-Ni^+(CO)$ binding energy is computed to be 21.5 kcal/mol.

Species **4** and **5** are connected by transition state $\mathbf{TS_{4-5}}$, which has been carefully confirmed by IRC calculations. The geometry of $\mathbf{TS_{4-5}}$ is largely similar to that of **4**, so it is an early transition state on the PES. Correspondingly, the relative energy of $\mathbf{TS_{4-5}}$ amounts to +1.1 kcal/mol, which translates into an activation barrier of 0.1 and 66.8 kcal/mol from **4** and **5**, respectively.

Nonreactive dissociation of the $(CH_4)-Ni^+(CO)$ bond of **5** would give rise to the decarbonylation products: $Ni^+(CO) + CH_4$. The overall decarbonylation process of $Ni^+(^2D) + CH_3CHO \rightarrow CH_4 + Ni^+(CO)$ is calculated to be exothermic by 44.2 kcal/mol. Note that the alternative channel for producing $Ni^+(CH_4)$ and CO is also exothermic (by 26.9 kcal/mol), though it was not detected in the ion beam experiment.[7]

We now turn to the alternative C−H activation branch for formation of the hydride-containing species **4**. This possibility involves the initial *trans*-**1** complex, followed by insertion of Ni^+ into the aldehyde C−H bond leading to species **3**, the C−H insertion minimum. Structurally, **3** ($^2A'$) is featured by an overall C_s symmetry with $O-C^1-C^2-Ni^+$ as the symmetry plane as well as by the rupture of the aldehyde C−H bond and the formation of the Ni^+-H bond as reflected by the corresponding bond lengths. Energetically, species **3** is calculated to be 19.5

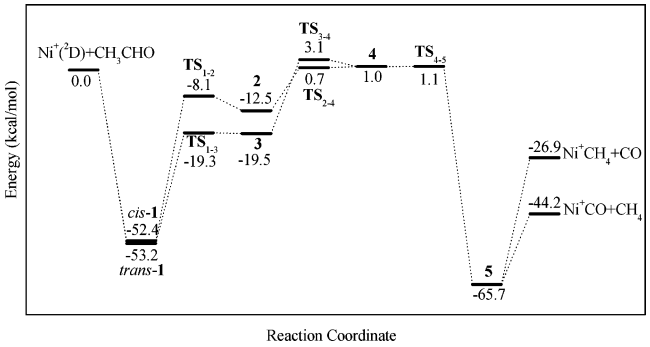

Figure 2. Calculated reaction branches of the (Ni, O, C_2, H_4)$^+$ PES at the B3LYP/6-311+G(2df,2pd) level of theory. All the relative energies are reported with ZPE corrections with the scaling factor of 0.955.[2]

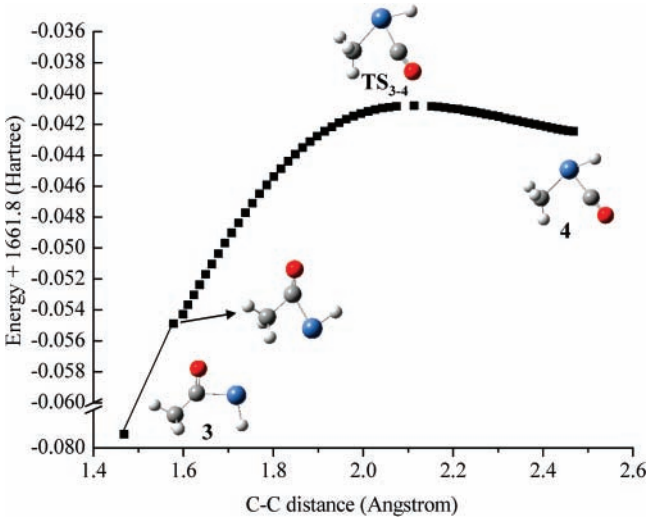

Figure 3. Selected structures as well as potential energy surface (PES) from the IRC calculations starting with transition state $\mathbf{TS_{3-4}}$ at the B3LYP/6-311+G(2df,2pd) level of theory.

kcal/mol below the separated reactants, or 7.0 kcal/mol more stable than the corresponding C−C insertion minimum **2**.

$\mathbf{TS_{1-3}}$ constitutes the first-order saddle point of the C−H activation process as confirmed by the transition vector associated with an imaginary frequency of 377*i* cm^{-1}. This transition state is expected to be very "late" along the reaction coordinate because it bears already a large structural similarity to species **3** as well as lying only 0.2 kcal/mol above **3**. It is interesting to note that the energy barrier of the C−H activation is 11.2 kcal/mol lower than that for the C−C activation, suggesting that aldehyde C−H activation is indeed more feasible in the gas-phase reaction of Ni^+ with acetaldehyde.

It is important to note that the C−H insertion intermediate **3** can also convert into the hydride-containing species **4** through transition state $\mathbf{TS_{3-4}}$ as suggested by the vibration vector of the imaginary frequency (195*i* cm^{-1}) that corresponds to the breaking of the C−C bond as well as by the intrinsic IRC as shown in Figure 3. This possibility is analogous to the situation of $^6Fe^+ + CH_3CHO$ as discussed below but different from that of Cr^+, Co^+, and $^4Fe^+ + CH_3CHO$.[1,2] Energetically, the transition state is calculated to be 3.1 kcal/mol above the separated reactants, or 2.4 kcal/mol higher than the corresponding transition state along the C−C activation pathway ($\mathbf{TS_{2-4}}$).

In summary, for the Ni^+/CH_3CHO system, both C−C and aldehyde C−H insertions could lead to the hydride-containing species through two elementary steps, i.e., C−C insertion followed by aldhyde H-shift and aldehyde C−H insertion

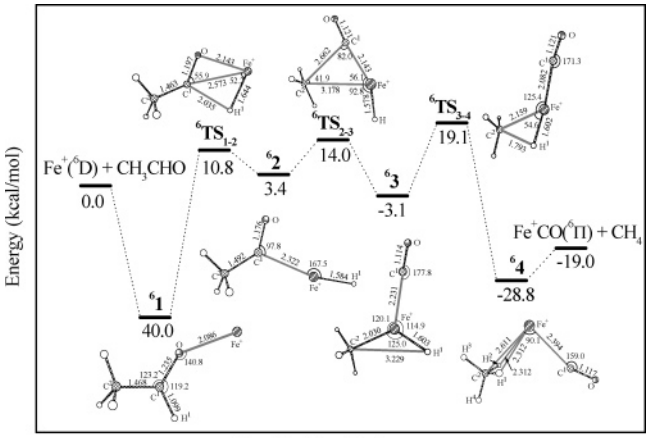

Figure 4. Calculated C−H activation reaction branch of the (^6Fe, O, C_2, H_4)$^+$ PES at the CCSD(T)/BSI//B3LYP/6-311+G(2df,2pd) level of theory, where BSI is the basis sets of 6-311+G(2df,2pd) for Fe and 6-311++G(d,p) for C, H, and O. All the relative energies are reported with ZPE corrections with the scaling factor of 0.955.[2] Bond lengths are in angstroms and bond angles in degrees.

followed by methyl shift. The energy for the first step of the C−H insertion pathway is lower than that for the C−C insertion, whereas for the second step the C−H insertion pathway is a little more energetically needed. Once the hydride-containing species is reached, it would convert into the decarbonylation precursor species readily. Nonreactive dissociation of the $(CH_4)-Ni^+(CO)$ bond of the precursor species would give rise to the exothermic products $Ni^+(CO) + CH_4$ as observed experimentally.[7]

The above-mentioned decarbonylation pathways show that the hydride-containing species is a common minimum that locates on both the routes of C−C and aldehyde C−H activation of acetaldehyde by metal ions. Considering the similarity that is held by the $^6Fe^+$ and Ni^+/CH_3CHO systems, we recalculated the aldehyde C−H activation pathway of the decarbonylation of $^6Fe^+ + CH_3CHO$ more carefully.[2] The corresponding PES, as well as the optimized structures, is shown in Figure 4 as a revision of our former work.[2] On the sextet C−H activation pathway, encounter complex $\mathbf{^61}$ can convert to the C−H insertion minimum of $\mathbf{^62}$ (E_{rel} = 3.4 kcal/mol) by passing through transition state $\mathbf{^6TS_{1-2}}$, which is calculated to locate at E_{rel} = 10.8 kcal/mol. Similar to the situation of the Ni^+/CH_3CHO system, species $\mathbf{^62}$ could convert into precursor complex $\mathbf{^64}$ through a two-step process: a C−C activation for the formation of the hydride-containing species $\mathbf{^63}$ and a hydride H-shift to form the precursor species $\mathbf{^64}$ (E_{rel} = −28.8 kcal/mol). The energy barriers for these two steps are calculated to locate at E_{rel} = 14.0 and 19.1 kcal/mol, respectively, the later of which makes it the crest along the reaction coordinate. Nonreactive dissociation of the $(CH_4)-{}^6Fe^+(CO)$ bond of $\mathbf{^64}$ would give rise to decarbonylaiton products: $FeCO^+$ ($^6\Pi$) + CH_4. Comparing with the PES for the C−C activation route,[2] we find that the aldehyde C−H activation mechanism is indeed more favorable for the decarbonylation of acetaldehyde mediated by Fe^+ (^6D, $3d^64s^1$).

We also explored the possibility for the C−H insertion species conversion to the precursor species in an H-shift concerted way for the other transition metal ions. However, we were unable to locate such a transition state that connects these minima in spite of our careful searches. We have thus discarded this route as a possible decarbonylation pathway for these metal ions.

4. Conclusions

The present theoretical work on the $Ni^+ + CH_3CHO$ reaction provides further insight into the mechanistic details of decarbonylation of acetaldehyde with late first-row transition metal ions. Combining with our previous studies concerning the reaction of the series of Cr^+-Fe^+ with acetaldehyde,[1,2] we can find that for the Cr^+, Co^+, and $^4Fe^+$ mediated systems decarbonylation of CH_3CHO only takes place via C−C activation, and aldehyde C−H activation is unlikely to be important. On the other hand, both C−C and aldehyde C−H activations could result in the decarbonylation of CH_3CHO with Ni^+ and $^6Fe^+$, where potential minimum $M^+(H)(CO)(CH_3)$ is located to be a common species on the decarbonylation pathways.

Acknowledgment. This work was supported by NCET-05-0608, Excellent Young Teachers Program, and Key Project (No. 104119) of MOE, P.R.C., National Natural Science Foundation of China (No. 20476061), and Natural Science Foundation of Shandong Province (No. Y2006B35).

References and Notes

(1) Zhao, L. M.; Zhang, R. R.; Guo, W. Y.; Wu, S. J.; Lu, X. Q. *Chem. Phys. Lett.* **2005**, *414*, 28.

(2) Zhao, L. M.; Guo, W. Y.; Zhang, R. R.; Wu, S. J.; Lu, X. Q. *ChemPhysChem* **2006**, *7*, 1345.

(3) Burnier, R. C.; Byrd, G. D.; Freiser, B. S. *Anal. Chem.* **1980**, *52*, 1641.

(4) Sonnenfroh, D. M.; Farrar, J. M. *J. Am. Chem. Soc.* **1986**, *108*, 3521.

(5) Burnier, R. C.; Byrd, G. D.; Freiser, B. S. *J. Am. Chem. Soc.* **1981**, *103*, 4360.

(6) Halle, L. F.; Crowe, W. E.; Armentrout, P. B.; Beauchamp, J. L. *Organometallics* **1984**, *3*, 1694.

(7) Tolbert, M. A.; Beauchamp, J. L. *J. Phys. Chem.* **1986**, *90*, 5015.

(8) Becke, A. D. *J. Chem. Phys.* **1993**, *98*, 1372.

(9) Lee, C.; Yang, W.; Parr, R. G. *Phys. Rev. B* **1988**, *37*, 785.

(10) (a) Chen, X. F.; Guo, W. Y.; Zhao, L. M.; Fu, Q. T. *Chem. Phys. Lett.* **2006**, *432*, 27. (b) Rodriguez-Santiago, L.; Noguera, M.; Sodupe, M.; Salpin, J. Y.; Tortajada, J. *J. Phys. Chem. A* **2003**, *107*, 9865. (c) Constantino, E.; Rimola, A.; Rodriguez-Santiago, L.; Sodupe, M. *New J. Chem.* **2005**, *29*, 1585. (d) Rodriguez-Santiago, L.; Tortajada, J. *Int. J. Mass Spectrom.* **2002**, *219*, 429. (e) Rodriguez-Santiago, L.; Sodupe, M.; Tortajada, J. *J. Phys. Chem. A* **2001**, *105*, 5340. (f) Corral, I.; Mo, O.; Yanez, M. *Theor. Chem. Acc.* **2004**, *112*, 298. (g) Galiano, L.; Alcami, M.; Mo, O.; Yanez, M. *ChemPhysChem* **2003**, *4*, 72. (h) Luna, A.; Alcami, M.; Mo, O.; Yanez, M.; Tortajada, J. *Int. J. Mass Spectrom.* **2002**, *217*, 119.

(11) Gonzalez, C.; Schlegel, H. B. *J. Phys. Chem.* **1990**, *94*, 5523.

(12) Glendening, E. D.; Reed, A. E.; Carpenter, J. E.; Weinhold, F. *NBO* Version 3.1.

(13) Reed, A. E.; Curtiss, L. A.; Weinhold, F. *Chem. Rev.* **1988**, *88*, 899.

(14) Foster, J. P.; Weinhold, F. *J. Am. Chem. Soc.* **1980**, *102*, 7211.

(15) Frisch, M. J.; Trucks, G. W.; Schlegel, H. B.; Scuseria, G. E.; Robb, M. A.; Cheeseman, J. R.; Montgomery, J. A., Jr.; Vreven, T.; Kudin, K. N.; Burant, J. C.; Millam, J. M.; Iyengar, S. S.; Tomasi, J.; Barone, V.; Mennucci, B.; Cossi, M.; Scalmani, G.; Rega, N.; Petersson, G. A.; Nakatsuji, H.; Hada, M.; Ehara, M.; Toyota, K.; Fukuda, R.; Hasegawa, J.; Ishida, M.; Nakajima, T.; Honda, Y.; Kitao, O.; Nakai, H.; Klene, M.; Li, X.; Knox, J. E.; Hratchian, H. P.; Cross, J. B.; Adamo, C.; Jaramillo, J.; Gomperts, R.; Stratmann, R. E.; Yazyev, O.; Austin, A. J.; Cammi, R.; Pomelli, C.; Ochterski, J. W.; Ayala, P. Y.; Morokuma, K.; Voth, G. A.; Salvador, P.; Dannenberg, J. J.; Zakrzewski, V. G.; Dapprich, S.; Daniels, A. D.; Strain, M. C.; Farkas, O.; Malick, D. K.; Rabuck, A. D.; Raghavachari, K.; Foresman, J. B.; Ortiz, J. V.; Cui, Q.; Baboul, A. G.; Clifford, S.; Cioslowski, J.; Stefanov, B. B.; Liu, G.; Liashenko, A.; Piskorz, P.; Komaromi, I.; Martin, R. L.; Fox, D. J.; Keith, T.; Al-Laham, M. A.; Peng, C. Y.; Nanayakkara, A.; Challacombe, M.; Gill, P. M. W.; Johnson, B.; Chen, W.; Wong, M. W.; Gonzalez, C.; Pople, J. A. *Gaussian 03*, revision B.05; Gaussian, Inc.; Pittsburgh, PA, 2003.

(16) Holthausen, M. C.; Fiedler, A.; Schwarz, H.; Koch, W. *J. Phys. Chem.* **1996**, *100*, 6236.

(17) Holthausen, M. C.; Koch, W. *J. Am. Chem. Soc.* **1996**, *118*, 9932.

(18) Yi, S. S.; Blomberg, M. R. A.; Siegbahn, P. E. M.; Weisshaar, J. C. *J. Phys. Chem. A* **1998**, *102*, 395.